Dalton Transactions

Cite this: *Dalton Trans.*, 2012, **41**, 5502

www.rsc.org/dalton

PAPER

Application of molybdenum *bis*(imido) complexes in ethylene dimerisation catalysis†

William R. H. Wright,[a,b] Andrei S. Batsanov,[b] Antonis M. Messinis,[a,b] Judith A. K. Howard,[b] Robert P. Tooze,[c] Martin J. Hanton*[c] and Philip W. Dyer*[a,b]

Received 29th October 2011, Accepted 12th December 2011
DOI: 10.1039/c2dt12061e

In combination with $EtAlCl_2$ (Mo : Al = 1 : 15) the imido complexes $[MoCl_2(NR)(NR')(dme)]$ (R = R′ = 2,6-Pr^i_2–C_6H_3 (**1**); R = 2,6-Pr^i_2–C_6H_3, R′ = Bu^t (**3**); R = R′ = Bu^t (**4**); dme = 1,2-dimethoxyethane) and $[Mo(NHBu^t)_2(NR)_2]$ (R = 2,6-Pr^i_2–C_6H_3 (**5**); R = Bu^t (**6**)) each show moderate TON, activity, and selectivity for the catalytic dimerisation of ethylene, which is influenced by the nature of the imido substituents. In contrast, the productivity of $[MoCl_2(NPh)_2(dme)]$ (**2**) is low and polymerisation is favoured over dimerisation. Catalysis initiated by complexes **1–4** in combination with $MeAlCl_2$ (Mo : Al = 1 : 15) exhibits a significantly lower productivity. Reaction of complex **5** with $EtAlCl_2$ (2 equiv.) gives rise to a mixture of products, while addition of $MeAlCl_2$ affords $[MoMe_2(N–2,6\text{-}Pr^i_2–C_6H_3)_2]$. Treatment of **6** with $RAlCl_2$ (2 equiv.) (R = Me, Et) yields $[Mo(\{\mu\text{-}N–Bu^t\}AlCl_2)_2]$ (**7**) in both cases. Imido derivatives **1** and **3** react with Me_3Al and $MeAlCl_2$ to form the bimetallic complexes $[MoMe_2(N\{R\}AlMe_2\{\mu\text{-}Cl\})(NR')]$ (R = R′ = 2,6-Pr^i_2–C_6H_3 (**8**); R = 2,6-Pr^i_2–C_6H_3, R′ = Bu^t (**10**)) and $[MoMe_2(N\{R\}AlCl_2\{\mu\text{-}Cl\})(NR')]$ (R = R′ = 2,6-Pr^i_2–C_6H_3 (**9**); R = 2,6-Pr^i_2–C_6H_3, R′ = Bu^t (**11**)), respectively. Exposure of complex **8** to five equivalents of thf or PMe_3 affords the adducts $[MoMe_2(N–2,6\text{-}Pr^i_2–C_6H_3)_2(L)]$ (L = thf (**12**); L = PMe_3 (**13**)), while reaction with NEt_3 (5 equiv.) yields $[MoMe_2(N–2,6\text{-}Pr^i_2–C_6H_3)_2]$. The molecular structures of complexes **5**, **9** and **11** have been determined.

Introduction

Selective transition metal-initiated alkene oligomerisation (in particular ethylene di- and trimerisation) has been the focus of a substantial industrial and academic research effort, providing simple and economical routes for the manufacture of higher olefinic feed stocks.[1–6] Of particular importance in this area is the manufacture of linear, terminal, short-chain materials (C_4–C_{20}) that are finding increasing uses as plasticiser co-monomers in polyethylene manufacture and as components of synthetic lubricant base oils.[7–9] A variety of different initiator systems have been developed for such applications, with those based on the Group 4, 6 and 10 metals being amongst the most successful and commercially relevant.[10–14]

Recent years have seen a particular resurgence of interest in oligomerisation systems incorporating Group 6 metals especially those utilising chromium and tungsten. For example, building upon the pioneering studies of Manyik *et al.* and subsequently those of Briggs, chromium-based systems bearing nitrogen-containing ligands for selective alkene oligomerisation have been extensively probed.[15–19] A wide variety of mono-, bi-, and tridentate metal scaffolds have been employed, with pyrrolyide-supported initiators proving especially important from an industrial perspective.[6,20] The success of these latter systems is, in part, due to the variable η^1-/η^5-coordination behaviour of the *aza*-heterocycle.[21] Notably, a related phenomenon has been reported for Cr(I) *bis*(diphenylphosphino)propane pro-initiators, which upon activation by alkyl aluminium reagents, form diphosphine-bridged *ansa*-*bis*(arene) Cr(I) species.[22] Together, these results highlight the potential importance of ligands that may adopt more than one binding mode (*i.e.* linkage isomerism) in the field of oligomerisation catalysis.

Attempts have also been made to utilise electronically-flexible *N*-donors to prepare chromium-based pro-initiators. Here efforts have focused on well-established imido ligands (NR^{2-}) that can behave as 2- or 4-electron metal scaffolds.[23–25] However, in combination with a variety of aluminium co-activators these chromium imido systems (*e.g.* $CrX_2(N–2,6\text{-}Pr^i_2–C_6H_3)_2$, X = Cl, Bu^t) yield high molecular weight polymer rather than the desired olefin oligomerisation products.[26]

In contrast, related tungsten imido complexes such as $[WCl_4(N–2,6\text{-}Pr^i_2–C_6H_3)(thf)]$ and $[WCl_2(N–2,6\text{-}Pr^i_2–C_6H_3)_2(dme)]$ are both active for selective ethylene and propylene dimerisation when treated with $EtAlCl_2$.[27,28] Importantly,

---

[a] *Centre for Sustainable Chemical Processes, Department of Chemistry, Durham University, South Road, Durham, UK, DH1 3LE. E-mail: p.w.dyer@durham.ac.uk; Fax: +44 (0) 191 334 2150; Tel: +44(0)191 384 4737*
[b] *Department of Chemistry, Durham University, South Road, Durham, UK, DH1 3LE*
[c] *Sasol Technology (UK) Ltd, Purdie Building, North Haugh, St Andrews, Fife, UK, KY16 9ST. E-mail: martin.hanton@eu.sasol.com*

† CCDC reference numbers 852768–852770. For crystallographic data in CIF or other electronic format see DOI: 10.1039/c2dt12061e

Table 1 Ethylene dimerisation using pre-formed molybdenum *bis*(imido) complexes **1–6**[a]

Pro-initiator	Activator	Time (min)	TON[b]	Activity[c]	Mol % C_4[d] (of liq. prod.)	% 1-C_4 in C_4	% PE
1	$EtAlCl_2$	55	58 500	63 820	88.9	63.7	0.1
1	$MeAlCl_2$	55	24 790	27 250	97.5	78.6	0.5
2	$EtAlCl_2$	1.5	770	34 350	94.1	97.9	69.6
2	$MeAlCl_2$	3	2020	47 250	83.2	97.5	20.5
3	$EtAlCl_2$	80	59 510	44 870	89.3	61.5	0.2
3	$MeAlCl_2$	9	4420	28 500	90.9	87.0	0.2
4	$EtAlCl_2$	74	14 030	11 360	88.9	63.7	3.0
4	$MeAlCl_2$	2	1790	48 660	81.5	94.1	18.5
5	$EtAlCl_2$	54	56 940	62 880	87.7	62.9	0.0
6	$EtAlCl_2$	4	120	1900	100.0	100.0	0.0

[a] General conditions: 0.2 mmol pro-initiator and 3.0 mmol $RAlCl_2$ (R = Me or Et); PhCl (solvent) 74 mL; 60 °C; ethylene pressure (40 bar); stirrer speed 1000 rpm; nonane standard (1.000 mL); catalytic runs were performed until consumption of C_2H_4 dropped below 0.2 g min^{-1}, at which time reaction was quenched by addition of dilute HCl. [b] TON is reported in (mol C_2H_4) (mol Mo)$^{-1}$. [c] Activity is reported in (mol C_2H_4) (mol Mo)$^{-1}$ h^{-1}. [d] In all runs C_6 alkenes were produced (8.4–9.8% of liquid products) as well as trace $\geq C_8$ fractions (0.1–2.4% of liquid products). PE = polyethylene.

these observations support the proposed role of tungsten imido species in selective olefin dimerisation catalysis mediated by commercially attractive initiator systems derived *in situ* from sequential reaction of inexpensive WCl_6 with aniline, triethylamine, and $EtAlCl_2$ (W : aniline : NEt_3 : Al 1 : 2 : 4 : 15).[29–33] These multi-component systems are not only extremely selective to the dimer products for a range of α-olefins (>99% *vs.* higher oligomers), but also demonstrate high specificity for methyl-branched products.

Despite the importance of both chromium- and tungsten-based initiators in catalytic olefin dimerisation, no studies have been reported that probe the potential of analogous molybdenum systems. This is surprising since the utility of Mo-containing complexes in olefin metathesis chemistry has lead to the preparation of a wide variety of variously-substituted molybdenum imido, derivatives, something that could open the way for detailed structure/property correlations to be established.[34–36] Furthermore, a number of well-defined molybdenum imido complexes are commercially available, making use of such systems attractive from an industrial perspective. Consequently, herein, we report a fundamental study of the reactivity of a number of readily accessible molybdenum imido complexes with alkyl aluminium reagents and explore their potential as pro-initiators in selective, catalytic ethylene dimerisation.

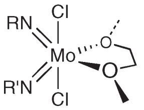

1: R = R' = 2,6-Pr^i_2-C_6H_3
2: R = R' = Ph
3: R = 2,6-Pr^i_2-C_6H_3, R' = Bu^t
4: R = R' = Bu^t

Results and discussion

Catalytic ethylene dimerisation testing

The utility of a series of readily accessible molybdenum imido complexes [$MoCl_2(NR)(NR')(dme)$] (R = R′ = 2,6-Pr^i_2–C_6H_3 (**1**);[37,38] R = R′ = Ph (**2**);[39] R = 2,6-Pr^i_2–C_6H_3, R′ = Bu^t (**3**);[40] R = R′ = Bu^t (**4**)[41]) as pro-initiators for ethylene dimerisation in combination with an aluminium activator $RAlCl_2$ (R = Me, Et) has been explored. Catalytic performance for each system was screened under conditions analogous to those used for the WCl_6-derived *in situ* systems, namely an Mo : Al ratio of 1 : 15, 40 bar ethylene pressure, and chlorobenzene as the solvent at 60 °C.[28,32]

In combination with $EtAlCl_2$ the pro-initiators **1**, **3**, and **4** each achieve a moderate selectivity to but-1-ene of ~90%, which compares favourably with the value established for the *in situ* WCl_6-derived system of ~80% (Table 1, Fig. 1).[32,42] A noticeable attenuation in the product selectivity is observed for the more active well-defined pro-initiators consistent with the incorporation of the higher olefinic products generated during catalysis. The activity of the pro-initiators **1–4** varied according to the nature of the imido substituents, decreasing in the order **1** > **3** > **2** ≫ **4**. However, a comparison of the TONs (turnover numbers) for each pro-initiator reveals that both complexes **1** and **3** perform well (~60 000 (mol C_2H_4) (mol Mo)$^{-1}$), while the lifetimes of the *bis*(Ph)- and *bis*(Bu^t)-imido systems **2** and **4** are extremely low. Notably, the phenyl imido-substituted complex **2** also exhibits a very low selectivity to dimer products, instead affording significant quantities of polyethylene. The rapid deterioration in performance observed for pro-initiators **2** and **4** has tentatively been attributed to steric factors that open alternative, but potentially different reaction pathways for these Ph- and Bu^t-substituted imido systems. Although the steric demands of

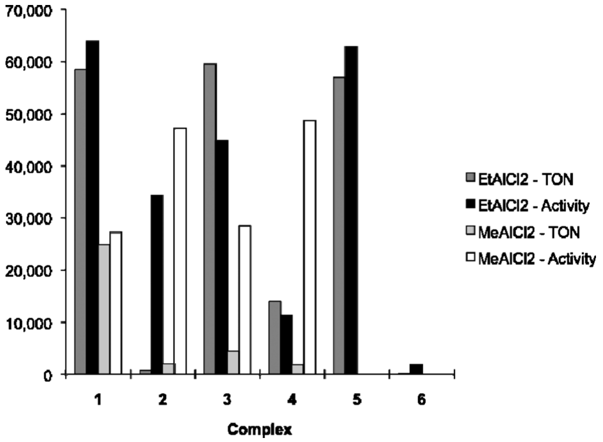

Fig. 1 Activity ((mol C_2H_4) (mol Mo)$^{-1}$ h^{-1}) and TON ((mol C_2H_4) (mol Mo)$^{-1}$) data for the dimerisation of ethylene initiated by complexes **1–6** in the presence of an aluminium activator (for experimental details see Table 1).

the N–Ph and N–Bu^t imido ligands are quite different, both motifs have a propensity to adopt bridging coordination modes, something that is prevented by the more sterically demanding N–2,6-Pr$^i_2$–C_6H_3 moiety (*vide infra*).[23]

Previously, deuterium labelling studies have indicated that olefin dimerisation mediated by tungsten *bis*(imido) pro-initiators (in combination with $EtAlCl_2$ as activator) most likely occurs *via* a chain-growth pathway. Such reactions are believed to proceed through a tungsten hydride species, which is generated *in situ* following β-hydride elimination from a tungsten ethyl group, itself resulting from Al-to-W transmetallation.[28,32] Adoption of this type of reaction manifold for tungsten systems is supported by the observation that replacing $EtAlCl_2$ by $MeAlCl_2$ as activator results in a very significant drop in catalytic performance.[32] Consequently, in order to probe the nature of the dimerisation path for molybdenum-based systems, the catalytic performance of complexes **1–4** was examined using $MeAlCl_2$ as activator. Although catalysis was initiated by each system, the productivities were significantly lower than those achieved using $EtAlCl_2$ as activator, although the levels of selectivity were retained (Table 1, Fig. 1). Together, these observations suggest that even when $MeAlCl_2$ is used tungsten hydride species are formed, albeit significantly less efficiently than with $EtAlCl_2$, as might be expected. Although the precise mechanistic trajectory by which $MeAlCl_2$ can lead to a metal hydride in such systems remains obscure, it could involve α-hydride elimination from a molybdenum or tungsten methyl species. Indeed, it is well known that for the WCl_6-based dimerisation systems use of lower loadings of aluminium activator results in a switch to an olefin metathesis pathway, although it should be noted that no metathesis products were detected in the catalysis performed here.[27]

Reactions of [Mo(NHBu^t)$_2$(NR)$_2$] with R'_xAlCl_{3-x}

Previous studies have clearly exemplified the participation of imido species in catalytic olefin dimerisation using *in situ* WCl_6/aniline-derived systems (*vide supra*). However, the potential role of amido-ligated (R_2N^-) species, which may equally as readily be generated during the formation of the active initiator, cannot be disregarded. Consequently, the catalytic performance of the mixed *bis*(amido) *bis*(imido) derivatives [Mo(NHBu^t)$_2$(NR)$_2$] (R = 2,6-Pr$^i_2$–C_6H_3 (**5**)[43] and R = Bu^t (**6**[44]) was explored in combination with $EtAlCl_2$ (15 equiv.) under identical reaction conditions. Here, use of the aryl imido complex **5** gave rise to a system that initiated dimerisation with activity, productivity, and selectivity that is identical to that for the analogous dichloride complex [$MoCl_2$(N–2,6-Pr$^i_2$–C_6H_3)$_2$(dme)] (**1**). In contrast, the *tert*-butyl imido derivative **6** was barely active, despite its parent complex [$MoCl_2$(NBu^t)$_2$(dme)] (**4**) exhibiting moderate activity.

To further probe the significant differences observed in the catalytic performance of the 2,6-Pr$^i_2$–C_6H_3- and Bu^t-substituted imido *tert*-butyl amido complexes **5** and **6**, respectively, their reactions with $EtAlCl_2$ were probed in detail. Treatment of diamide **6** with two equivalents of $EtAlCl_2$ in C_6D_6 solution cleanly afforded the previously reported bimetallic species [Mo({μ-N–Bu^t}$AlCl_2$)$_2$] (**7**) and ethane, the latter resulting from deprotonation of the parent diamide, eqn (1).[44] Notably, this imido-bridged complex **7** was found to be inert to further alkylation and did not react with ethylene (10 equiv.) even in the presence of excess $EtAlCl_2$. In contrast, reaction of complex **5** with $EtAlCl_2$ (2 equiv.) under identical conditions afforded a mixture of unassignable products (according to ^1H and ^{13}C NMR spectroscopy), although it was clear that no ethane evolution occurred. However, subsequent addition of ethylene (10 equiv.) to this complex mixture resulted in the formation of small quantities of butenes indicative of the presence of a dimerisation-active species.

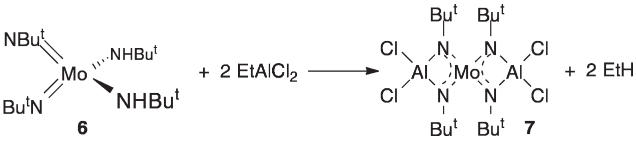

(1)

Analogous reactions of complexes **5** and **6** with $MeAlCl_2$ (2 equiv.) were carried out (C_6D_6 solution) in order to probe the potential role of ethyl group β-hydride elimination, Scheme 1. Again, complex **6** was subject to deprotonation and afforded **7** and methane, while derivative **5** cleanly gave the known dimethyl complex [$MoMe_2$(N–2,6-Pr$^i_2$–C_6H_3)$_2$] *via* transmetallation; the formation of methane was not observed for the latter reaction.[45,53]

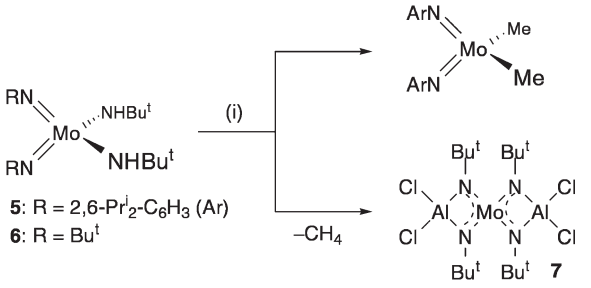

Scheme 1 (i) $MeAlCl_2$ (2 equiv.), C_6D_6, room temperature.

In order to explore the differences in reactivity determined for complexes **5** and **6**, attempts were made to determine their molecular structures. However, despite repeated attempts, no crystals of **6** suitable for X-ray diffraction studies could be obtained. In contrast, the molecular structure of complex **5** was verified by single-crystal X-ray diffraction (Fig. 2). This proved very similar to that of the previously reported complex [Mo(HN–2,6-Pr$^i_2$–C_6H_3)$_2$(N–2,6-Pr$^i_2$–C_6H_3)$_2$], with the Mo atom possessing a distorted tetrahedral coordination.[46]

As expected, the imido Mo–N bond distances (1.7609(14) and 1.7543(15) Å) in **5** are intermediate between those of an LX_2 ($4e^-$) and X_2 ($2e^-$) donor and, although the two Mo═N–C^{Ar} bond angles differ significantly (155.3(1) and 170.3(1)°), they lie within the accepted range for *quasi*-linear imido motifs (150–180°).[40] The Mo–N amido bond distances are comparable with other molybdenum amido complexes (1.92–2.15 Å).[46,47] Both amide nitrogen atoms N(3) and N(4) are planar, within experimental error, and are orientated such that the N(3)–Mo–N(4) plane and the H–N–C planes for N(3) and N(4) are at 62.7 and 70.6°, respectively. This arrangement maximises the extent of N(pπ)→Mo(dπ) donation for each amido ligand about the *pseudo*-tetrahedral Mo atom, something facilitated by the

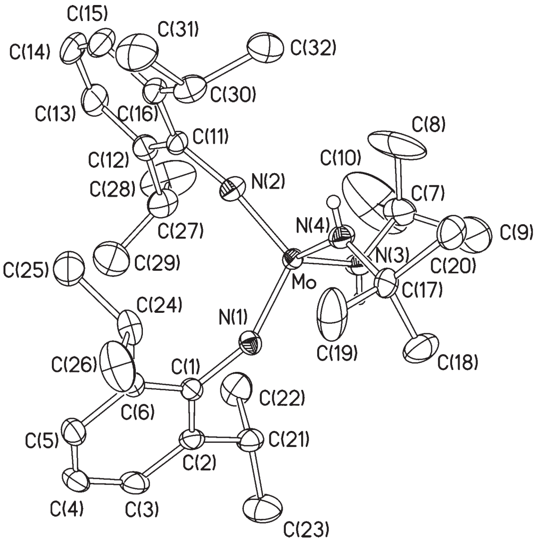

Fig. 2 Molecular structure of [Mo(NHBu^t)$_2$(N–2,6-Pr$^i_2$–C$_6$H$_3$)$_2$] (**5**). H atoms are omitted for clarity and the thermal ellipsoids are shown at the 50% level. Selected bond distances (Å) and angles (°): Mo–N(1) 1.7609 (14), Mo–N(2) 1.7543(15), Mo–N(3) 1.9537(16), Mo–N(4) 1.9495(16), N(1)–Mo–N(2) 112.32(7), N(3)–Mo–N(4) 111.88(7), N(1)–Mo–N(3) 105.53(7), N(1)–Mo–N(4) 111.25(7), Mo–N(1)–C(1) 155.32(13), Mo–N(2)–C(11) 170.28(13), Mo–N(3)–C(7) 130.80(14), Mo–N(4)–C(17) 133.68(13). Neither amido ligand forms any hydrogen bonds.

pseudo-trans disposition of the two Bu^t substituents, which reduces steric constraints.[48–50]

These solid-state data emphasize the electron-withdrawing nature of the aryl imido ligands, evidenced by appreciable N$_{\text{amido}}$→Mo lone pair donation. This is consistent with the ^{1}H NMR spectrum of complex **5** in which the amido NH proton appears to considerably higher frequency to that for complex **6** bearing electron-releasing *tert*-butyl imido ligands, δ 6.29 (**5**)[44] *versus* 5.71 ppm (**6**). Further corroboration of this electronic disparity is given by a comparison of the chemical shift difference between the α and β carbon resonances ($\Delta\delta$) of the *tert*-butyl amido substituents of **5** ($\Delta\delta$ = 22.1 ppm) and **6** ($\Delta\delta$ = 19.6 ppm). By analogy with the use of this parameter to probe the electron density at the imido nitrogen atom of d^0 *tert*-butyl imido complexes, the greater magnitude of $\Delta\delta$ for complex **5** is consistent with lower electron density at its amido nitrogen atoms, again resulting from greater N$_{\text{amido}}$→Mo donation. Together, these data are all indicative of a superior acidity of the amido NH group of **5** *versus* that of **6**.[51] However, this clear difference in electronic nature of the imido substituents and consequently, in the relative acidities of the NH moieties of complexes **5** and **6**, does not correlate with their observed reactivity with RAlCl$_2$ (R = Et, Me) since only the less acidic amido group of **6** is subject to deprotonation. Consequently, it is likely that the greater steric demands of the 2,6-diisopropylphenyl substituents of **5** prevent the formation of imido-bridged dimeric species such as **7**, which result from amido deprotonation. Thus, the poor catalytic performance of pro-initiator **6** in combination with the necessary alkyl aluminium activator is attributed to the formation of complex **7** *in situ*, which prevents access to the catalytically productive manifold and highlights the probable role of similarly-bridged imido species in catalyst deactivation pathways.

Reactions of [MoCl$_2$(NR)(NR′)(dme)] with Me$_x$AlCl$_{3-x}$

Understanding the subtle interplay between aluminium activator and transition metal pro-initiator remains key to the elucidation of the mechanism of catalytic olefin dimerisation. For example, it has been proposed from computational studies that coordination of R′AlCl$_2$ to tungsten *bis*(imido) fragments enhances ethylene dimerization *via* an oxidative coupling pathway due to a lowering of the energy barrier for reductive elimination.[52] However, in a separate study, it has been revealed that although coordination of various Me$_x$AlCl$_{3-x}$ species to tungsten *bis* (imido) moieties does indeed take place, the resulting bimetallic systems are inert towards both ethylene and propylene.[28] Hence, given the differences observed in catalytic performance between the different molybdenum imido complexes **1–4**, the reactivity of each system with variously-substituted alkyl aluminium reagents has been studied.

Treatment of [MoCl$_2$(N–2,6-Pr$^i_2$–C$_6$H$_3$)$_2$(dme)] (**1**) with excess Me$_3$Al (6 equiv.) in hexane solution resulted in full conversion (by NMR spectroscopy) to [MoMe$_2$(N{2,6-Pr$^i_2$–C$_6$H$_3$}AlMe$_2${μ-Cl})(N–2,6-Pr$^i_2$–C$_6$H$_3$)] (**8**), Scheme 2. Here, the Me$_2$AlCl generated *in situ* by Al/Mo transmetallation has been sequestered by one of the Lewis basic imido nitrogens, presumably *via* an intermolecular pathway. In a similar fashion treatment of **1** with MeAlCl$_2$ (3 equiv.) in toluene cleanly afforded [MoMe$_2$(N{2,6-Pr$^i_2$–C$_6$H$_3$}AlCl$_2${μ-Cl})(N–2,6-Pr$^i_2$–C$_6$H$_3$)] (**9**), although further addition of MeAlCl$_2$ yielded other (unidentified) reaction products.‡ Complex **8** can also be formed directly *via* reaction of [MoMe$_2$(N–2,6-Pr$^i_2$–C$_6$H$_3$)$_2$] with Me$_2$AlCl, although the reaction also affords a significant number of other, unidentified side-products, eqn (2).

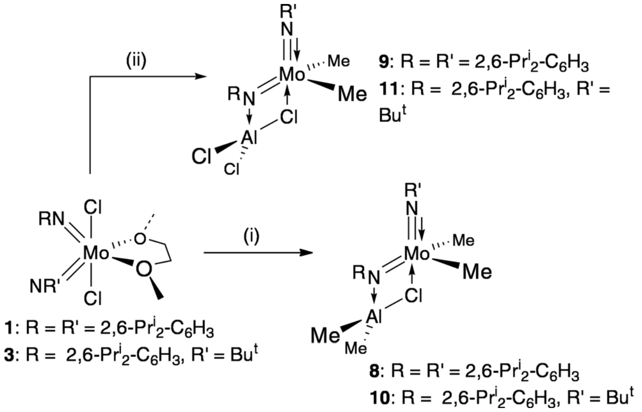

Scheme 2 (i) Me$_3$Al (6 equiv.), hexane, room temperature (r.t.); (ii) MeAlCl$_2$ (3.25 equiv.), toluene, r.t.

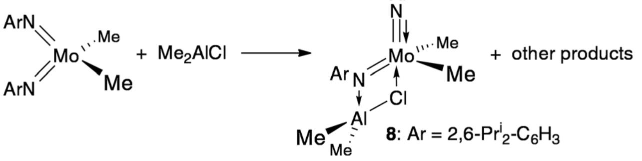

The ^{1}H NMR spectrum of **8** is consistent with the presence of a symmetrical MoMe$_2$ motif, which gives rise to a single resonance at δ 1.64 ppm, with the AlMe$_2$ moiety presenting a signal

Table 2 Selected bond distances (Å) and angles (°) for complexes **9** and **11**

	9, *A*	**9**, *B*	**9**, *C*	**9**, *D*	**9**, mean	**11**
Mo–Cl(1)	2.695(2)	2.708(2)	2.712(2)	2.695(2)	2.702(9)	2.7474(5)
Mo–N(1)	1.711(5)	1.718(5)	1.712(5)	1.723(5)	1.716(6)	1.7024(14)
Mo–N(2)	1.891(6)	1.851(6)	1.867(6)	1.865(6)	1.869(16)	1.8874(13)
Mo–C(1)	2.136(7)	2.123(7)	2.126(7)	2.127(7)	}2.124(11)	2.1191(17)
Mo–C(2)	2.141(6)	2.118(7)	2.118(7)	2.106(7)		2.1217(17)
Mo···Al	3.054(2)	3.056(2)	3.058(2)	3.045(2)	3.053(6)	3.1024(6)
Al–Cl(1)	2.205(3)	2.195(3)	2.194(3)	2.198(3)	2.198(5)	2.1887(7)
Al–N(2)	1.878(5)	1.885(6)	1.893(6)	1.880(6)	1.884(7)	1.8718(14)
Al–Cl(2)	2.087(3)	2.091(3)	2.096(4)	2.107(3)	} 2.099(9)	2.1094(7)
Al–Cl(3)	2.109(3)	2.110(3)	2.089(3)	2.099(3)		2.1118(8)
Mo–N(1)–C	162.6(5)	163.1(5)	164.2(5)	164.3(5)	163.6(8)	174.6(1)
Mo–Cl(1)–Al	76.39(8)	76.33(8)	76.31(8)	76.30(8)	76.33(4)	76.96(2)
Mo–N(2)–Al	108.2(3)	109.8(3)	108.9(3)	108.8(3)	108.9(7)	111.23(6)
Mo–N(2)–C(11)	129.4(4)	130.6(4)	131.7(4)	131.8(4)	131(1)	127.4(1)
Al–N(2)–C(11)	122.3(5)	119.6(4)	119.4(5)	119.3(4)	120(1)	121.4(1)
Interplanar angle						
i/iii	10.4(3)	5.3(3)	4.1(3)	6.8(3)	6.7	—
ii/iii	86.6(1)	88.7(1)	88.2(2)	88.3(2)	87.9	89.0(1)

at δ − 0.09 ppm. Notably, the protons of the Mo–Me groups of **8** resonate to higher frequency of those reported previously for $[MoMe_2(N\text{–}2,6\text{-}Pr^i_2\text{–}C_6H_3)_2]$ (δ 1.39 ppm), consistent with the electron-withdrawing effect of the coordinated Me_2AlCl.[53] Analogously, the ^{13}C NMR spectrum for **8** shows two metal-bonded carbons at δ 41.5 and −7.0 ppm (Mo–Me and Al–Me, respectively), as expected. The ^1H NMR spectrum for complex **9** revealed a resonance at δ 1.67 ppm for the Mo–Me motif at a shift comparable to that determined for **8**.

With the aim of better understanding the crucial alkyl aluminium chloride–metal imido interaction, single crystals of complex **9** were grown from CH_2Cl_2 solution and characterised by X-ray diffraction (Fig. 3, Table 2). The asymmetric unit of **9**·½CH_2Cl_2 comprises four host molecules (A to D) of similar geometry, as well as two dichloromethane molecules (one of them chaotically disordered). The molecular structure of **9** reveals one terminal imido ligand, $N(1)\text{–}2,6\text{-}Pr^i_2\text{–}C_6H_3$ (mean Mo–N distance 1.715(6) Å) and an asymmetrically-bridged imido unit, together an arrangement that closely resembles that of the related tungsten complex $[WMe_2(N\{2,6\text{-}Pr^i_2\text{–}C_6H_3\}AlCl_2\{\mu\text{-}Cl\})(N\text{–}2,6\text{-}Pr^i_2\text{–}C_6H_3)]$.[28] The Mo atom of **9** adopts a trigonal-bipyramidal coordination distorted in an ‘umbrella’ fashion,[54] whereby the equatorial ligands (bridging $N(2)\text{–}2,6\text{-}Pr^i_2\text{–}C_6H_3$ and two methyl groups) are pushed away from the terminal Mo–N(1) bond and towards the bridging chloride ligand. The latter is rather weakly bonded, the Mo–Cl distance being longer even than previously reported Ar–Cl→Mo dative bonds (2.581(5) or 2.624(1) Å).[55] The Al atom of **9** adopts a near-tetrahedral geometry, with N(2) being trigonal planar (mean Σ_{ang} N(2) ~ 360°). Arene ring (i) is roughly coplanar with the MoN(2)AlCl metallacycle (iii), while ring (ii) adopts a perpendicular orientation.

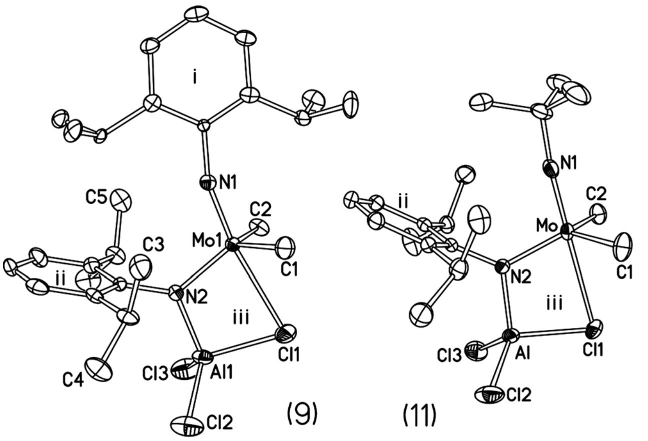

Fig. 3 Molecular structures of $[MoMe_2(N\{2,6\text{-}Pr^i_2\text{–}C_6H_3\}AlCl_2\{\mu\text{-}Cl\})(N\text{–}2,6\text{-}Pr^i_2\text{–}C_6H_3)]$·½$CH_2Cl_2$ (**9**)—independent molecule *A* only, and $[MoMe_2(N\{2,6\text{-}Pr^i_2\text{–}C_6H_3\}AlCl_2\{\mu\text{-}Cl\})(NBu^t)]$ (**11**). H atoms are omitted for clarity and the thermal ellipsoids are shown at the 50% level.

The test data reported in Table 1 and Fig. 1 reveal a marked similarity in the catalytic performance of the *bis*(aryl) imido pro-initiator **1** and the mixed aryl/*tert*-butyl *bis*(imido) complex **3**, while those for the *bis*(Bu^t) imido complex **4** were significantly poorer. Thus, it was of interest to examine in detail the interplay between the mixed imido complex $[MoCl_2(N\text{–}2,6\text{-}Pr^i_2\text{–}C_6H_3)(NBu^t)(dme)]$ (**3**) and $Me_xAlCl_{(3-x)}$ reagents. As was the case for **1**, reaction of **3** with Me_3Al (6 equiv.) or $MeAlCl_2$ (3 equiv.) in toluene smoothly afforded the Lewis acid-containing complexes $[MoMe_2(N\{2,6\text{-}Pr^i_2\text{–}C_6H_3\}AlX_2\{\mu\text{-}Cl\})(NBu^t)]$ where X = Me (**10**) and X = Cl (**11**), respectively, Scheme 2.‡ Consistent with the proposed structure, complex **10** exhibits both Mo–Me and Al–Me resonances in its ^1H (δ 1.39 and −0.21 ppm, respectively) and ^{13}C (δ 39.3 and −6.7 ppm, respectively) NMR spectra. The regiochemistry of complex **10** was confirmed *via* a $^1H/^1H$ NOESY experiment, which revealed a unique correlation between the Me groups of the $2,6\text{-}Pr^i_2\text{-}C_6H_3$ moiety and those bound to aluminium, consistent with a static structure in which there is coordination of Me_2AlCl to the aryl imido nitrogen only. Comparable NMR spectroscopic data were recorded for the Mo-methyl groups of complex **11** (^1H δ 1.38; ^{13}C δ 45.1 ppm). The weaker Lewis acidity of the bound $AlMe_2$ residue compared to that of the $AlCl_2$ unit is reflected in the values of $\Delta\delta$ associated with the *tert*-butyl imido ligands of complexes **10** (45.6 ppm) and **11** (48.2 ppm), respectively, which indicate greater $N_{imido}\rightarrow$ Mo lone pair donation for the latter.[51]

Recrystallisation of complex **11** from toluene afforded light yellow crystals suitable for an X-ray diffraction study. The structure contains one independent molecule (Fig. 3, Table 2) geometrically similar to **9**, except that the Mo–N–C bond angle of the terminal imido ligand in **11** is greater, presumably as a result of steric constraints.[56] The trigonal bipyramidal coordination of the Mo centre exhibits a comparable 'umbrella-type' distortion to that observed for **9**, with the Mo atom being displaced from the N(2)C(1)C(2) plane towards N(1) by 0.31 Å (*cf.* 0.35 Å in **9**). Specific coordination of the $AlCl_3$ moiety only to the aryl imido nitrogen N(2) rather than the *tert*-butyl imido nitrogen is apparent, which is in agreement with the inferences made for the analogous Me_2AlCl derivative **10** by NMR spectroscopy. As determined for complex **9**, the aluminium-bound nitrogen N(2) in **11** is trigonal planar (Σ_{ang} N(2) 359.95°).

Complexes **9** and **11** result from regioselective coordination of the Me_xAlCl_{3-x} ($x = 0$ or 2), generated *in situ* following transmetallation, to the aryl imido ligand of the $[MoMe_2(N–2,6\text{-}Pr^i_2–C_6H_3)(NBu^t)]$ fragment. The regioselectivity obtained here is consistent with observations that can be made from the molecular structure determination of the parent complex $[MoCl_2(N–2,6\text{-}Pr^i_2–C_6H_3)(NBu^t)(dme)]$ (**3**). Here, the Mo–N bond distance associated with the NBu^t ligand is significantly shorter than that for the aryl imido ligand (1.728(2) *vs.* 1.753(2) Å), which reflects the greater π-donation of the NBu^t lone pair to the molybdenum centre.[57] Consequently, this suggests that in complexes **9** and **11** the NBu^t imido lone pair is likely to be less available for donation to the Lewis acidic Me_xAlCl_{3-x} fragments, giving rise to the observed regiochemistry in the bimetallic complex.

Reactions of $[MoMe_2(N\{2,6\text{-}Pr^i_2–C_6H_3\}AlMe_2\{\mu\text{-}Cl\})(N–2,6\text{-}Pr^i_2–C_6H_3)]$ with Lewis bases

It has been established previously that tungsten imido-bound Al(III) species may be readily displaced through reaction with an appropriate Lewis base to afford the corresponding acid-free imido complexes, something that is of particular importance for the application of these molybdenum imido systems in olefin dimerisation.[28] Consequently, the reactivity of complex **8** with a variety of strong Lewis bases was probed in d_6-benzene and d_5-chlorobenzene solution (Scheme 3). Treatment of **8** with excess thf or PMe_3 (5 equiv.) cleanly afforded the known complexes $[MoMe_2(N–2,6\text{-}Pr^i_2–C_6H_3)(L)]$ (L = thf (**12**); L = PMe_3 (**13**) together with the corresponding base adducts $[Me_2AlCl(L)]$, while reaction of **8** with NEt_3 (5 equiv.) afforded the previously reported base-free complex $[MoMe_2(N–2,6\text{-}Pr^i_2–C_6H_3)_2]$.[28,53] In contrast, no reaction occurred either between **8** or even its base-free analogue, $[MoMe_2(N–2,6\text{-}Pr^i_2–C_6H_3)_2]$, and ethylene (5 equiv.) in C_6D_5Cl or C_6D_6 even at elevated temperature (60 °C), something that has been ascribed to the poor nucleophilicity of the olefin.

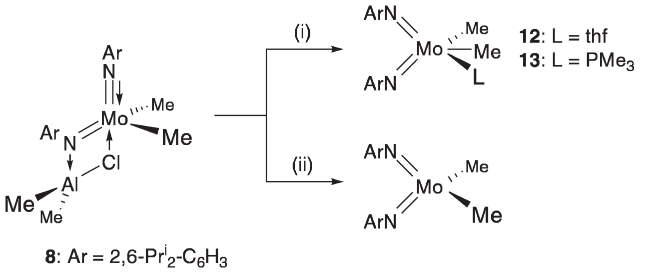

Scheme 3 (i) thf (5 equiv.) or PMe_3 (5 equiv.), C_6D_6, room temperature (r.t.); (ii) NEt_3 (5 equiv.), C_6D_6, r.t.

Analogous reactions with Lewis bases were attempted for the mixed *bis*(imido) complex **10**. As was the case with **8** (d_6-benzene solution) no reaction was found to occur with excess ethylene, while reactions with thf, PMe_3 and NEt_3 (5 equiv.) afforded unattributable mixtures of products. This latter observation has been ascribed to the occurrence of imido ligand exchange, something that was reported during attempts to prepare the base-free complex $[MoMe_2(N–2,6\text{-}Pr^i_2–C_6H_3)(NBu^t)]$.[53]

Conclusions

We have shown in this study that preformed molybdenum *bis*(imido) complexes bearing at least one bulky $2,6\text{-}Pr^i_2–C_6H_3$ substituent, in combination with alkyl aluminium dichlorides $RAlCl_2$ (R = Me, Et), exhibit moderate activity and productivity for ethylene dimerisation. Here, it is believed that the sterically-demanding imido ligand is required to inhibit imido bridge formation, something that can not only prevent access to a catalytically productive manifold during pro-initiator activation, but is also a major contributing factor to initiator degradation.

Additionally, it is noted that the catalytic performance of such *bis*(imido) molybdenum systems is intimately linked to the nature of the aluminium activator, with the highest productivities and selectivities being achieved with $EtAlCl_2$. It is proposed that the significantly better catalytic performance observed when using $EtAlCl_2$ (compared with $MeAlCl_2$) can be attributed to ready access to a molybdenum hydride-based catalytic manifold as a result of β-hydride elimination in the molybdenum coordination sphere following Et–Al to Et–Mo transmetallation.

In contrast, the low levels of catalytic dimerisation activity determined for the $MoCl_2(NR)_2/MeAlCl_2$ systems is proposed to result from the formation of low concentrations of Mo–H species *via* a much less accessible α-hydride abstraction pathway. These proposed mechanistic differences are supported by the observation that although Me-group transmetallation from $MeAlCl_2$ to d^0 molybdenum *bis*(imido) complexes is facile, the resulting new aluminium(III) species are sequestered by one of the Lewis basic imido nitrogen atoms to afford bimetallic complexes $[MoMe_2(N\{R\}AlMe_2\{\mu\text{-}Cl\})(NR')]$ (**8–11**), which do not initiate ethylene dimerisation at low ethylene concentrations. Moreover, no reaction is observed between ethylene and the base-free derivative $[MoMe_2(N–2,6\text{-}Pr^i_2–C_6H_3)_2]$ consistent with both the low nucleophilicity of the olefin and its low intrinsic kinetic facility for insertion. Together these observations are in agreement with studies of related aluminium-tungsten systems, which have also been demonstrated to be inert towards olefins, despite computational studies having highlighted such systems as potentially playing a crucial role in WCl_6/aniline-mediated olefin dimerisation.[28,52]

Further studies exploring the behaviour of Group 6 imido complexes in alkene dimerisation are on-going.

Experimental

All operations were conducted under an atmosphere of dry nitrogen using standard Schlenk and cannula techniques, or in a nitrogen-filled Saffron Scientific glove box. NMR-scale reactions were conducted using NMR tubes fitted with Young's tap valves. Bulk solvents were purified using an Innovative Technologies SPS facility and degassed prior to use and NMR solvents (C_6D_6) were dried over P_2O_5, distilled and degassed before use. When appropriate, liquid reagents were dried, distilled and deoxygenated. Nitrogen gas was passed through a drying column (silica–$CaCO_3$–P_2O_5). The known complexes $[MoCl_2(N\text{–}2,6\text{-}Pr^i_2\text{–}C_6H_3)_2(dme)]$ (**1**),[37,38] $[MoCl_2(NPh)_2(dme)]$ (**2**),[39] $[MoCl_2(N\text{–}2,6\text{-}Pr^i_2\text{–}C_6H_3)(NBu^t)(dme)]$ (**3**),[40] $[MoCl_2(NBu^t)_2(dme)]$ (**4**),[41] $[Mo(NHBu^t)_2(NBu^t)_2]$ (**6**)[44] were prepared using standard literature procedures, while neat Me_3Al was purchased from Albermarle R & D centre and $EtAlCl_2$ from Aldrich. Solid $MeAlCl_2$ was obtained by slow evaporation of hexane from a hexane solution obtained from Aldrich. $LiNHBu^t$ was prepared through addition of equimolar quantities of Bu^nLi to a cold (−78 °C) Et_2O solution of $HNBu^t$. Routine NMR spectra were collected on a Varian Unity 300 or 200, a Varian Mercury 400, Avance 400 MHz Bruker, Varian Inova 500, or a Varian 700 MHz spectrometers. Chemical shifts were referenced to residual protio impurities in the deuterated solvent (^1H) or the ^{13}C shift of the solvent. Solvent proton shifts (ppm): C_6D_6, 7.15. Solvent carbon shifts (ppm): C_6D_6, 128.3. Elemental analyses were performed by the Analytical Services Department of the Chemistry Department, Durham University.

Catalysis was performed in 250 mL volume Buchi Miniclaves equipped with stainless steel vessels with integral thermal-fluid jackets, internal cooling coils, and mechanical mixing *via* gas-entraining stirrers. Ethylene (Grade 4.5) was supplied by Linde and passed through oxygen and moisture scrubbing columns prior to use; ethylene flow was measured using a Siemens Sitrans F C Massflo system (Mass 6000–Mass 2100) and the data logged. All catalytic tests were allowed to run until ethylene uptake had dropped below the 0.2 g min^{-1} lower detection threshold. Gas phase sample GC-FID analysis was performed using an Agilent Technologies 6890 N GC System equipped with a 250 μL gas sample loop and GS GasPro column (30 m × 0.32 mm) using hydrogen as carrier gas. Liquid phase sample, GC-FID analysis was performed using an Agilent Technologies 6850 N GC System equipped with a PONA column (50 m × 0.20 mm × 0.50 μm) using hydrogen as carrier gas.

General procedure for evaluating ethylene dimerisation activity of pro-initiators 1–6

The autoclave was heated under vacuum at 90 °C for 1 h, then cooled and back-filled with Ar, before charging with PhCl (70 mL) and the required pro-initiator (20 μmol, as a 5 mM stock solution in PhCl). The vessel was then heated (60 °C), pressurized with ethylene (5 bar), and stirred (1000 rpm). Next, the autoclave was vented to enable addition of the desired activator, $EtAlCl_2$ or $MeAlCl_2$ (300 μmol). After activator addition, the vessel was pressurized with ethylene (40 bar). A constant pressure of 40 bar was maintained throughout the reaction period, whilst ethylene consumption was monitored *via* a flowmeter. After gas uptake was observed to cease, the autoclave was isolated from the ethylene supply and cooled to 0 °C. The reactor was carefully vented, with a portion of the vent gas being directly fed to a GC-FID instrument equipped with gas-sampling loop for analysis. Next, the reactor contents were treated sequentially with 1000 μL of nonane (GC internal standard) and a 10% aqueous HCl solution. A sample of the organic phase was taken for GC-FID analysis. Any solid formed was collected, washed repeatedly with 10% HCl and EtOH, dried overnight and weighed.

$[Mo(NHBu^t)_2(N\text{–}2,6\text{-}Pr^i_2\text{–}C_6H_3)_2]$ (5). To a cold (−78 °C) Et_2O (30 mL) solution of $[MoCl_2(N\text{–}2,6\text{-}Pr^i_2\text{–}C_6H_3)_2(dme)]$ (**1**) (2.0 g, 3.28 mmol) was added a cold (−78 °C) Et_2O (100 mL) solution of $LiNHBu^t$ (0.52 g, 6.57 mmol). The mixture was allowed to warm to r.t. and allowed to stir for a further 4 h. All volatile components were removed *in vacuo* and the residue extracted with hexane (3 × 30 mL) *via* filtration. Concentration of the resulting hexane solution under reduced pressure and subsequent recrystallisation at −35 °C afforded **5** as orange single crystals (0.36 g, 20%). Further concentration of the hexane solution resulted in precipitation of further quantities of **5** as an orange powder, which was collected by filtration; yield 0.45 g (45%). ^1H NMR ($CDCl_3$, 200 MHz): δ 6.96 (6H, br, H_{meta} and H_{para}), 6.29 (2H, br, N*H*), 3.57 (4H, septet, $^3J_{HH}$ = 6.8 Hz, CH_3CH), 1.29 (18H, s, $NCCH_3$), 1.11 (24H, d, $^3J_{HH}$ = 6.8 Hz, CH_3CH). $^{13}C\{^1H\}$ NMR ($CDCl_3$, 125.6 MHz): δ 153.5 (C_{ipso}), 140.5 (C_{ortho}), 123.3 (C_{meta}), 122.1 (C_{para}), 55.2 ($NCCH_3$), 33.1 ($NCCH_3$), 28.3 (CH_3CH), 23.1 (CH_3CH). Anal. calcd for $C_{32}H_{54}MoN_4$: C, 65.06; H, 9.21; N, 9.48. Found C, 65.00; H, 9.34; N, 9.58.

$[Mo(\{\mu\text{-}NBu^t\}_2AlCl_2)_2]$ (7).[44] $[Mo(NHBu^t)_2(NBu^t)_2]$ (**6**) (50 mg, 0.13 mmol) was dissolved in C_6D_6 (0.8 mL), $EtAlCl_2$ (34 mg, 0.26 mmol) added and the reaction monitored by ^1H NMR spectroscopy. Within 10 min quantitative formation of previously reported complex **7** and ethane had occurred. ^1H NMR (C_6D_6, 500 MHz): δ 1.38 (s, NBu^t), 0.71 (s, C_2H_6).

Reaction of $[Mo(NHBu^t)_2(N\text{–}2,6\text{-}Pr^i_2\text{–}C_6H_3)_2]$ with $EtAlCl_2$ and C_2H_4. $[Mo(NHBu^t)_2(N\text{–}2,6\text{-}Pr^i_2\text{–}C_6H_3)_2]$ (**5**) (50 mg, 0.08 mmol) was dissolved in C_6D_6 (0.8 mL), $EtAlCl_2$ (22 mg, 0.17 mmol) added and the reaction monitored by ^1H NMR spectroscopy, which indicated the formation of a number of unattributable products. Subsequently, the NMR tube and its contents were cooled (−196 °C), evacuated, and ethylene (10 equiv., 0.80 mmol) added, which lead to the formation of butenes according to ^1H NMR spectroscopy.

Reaction of $[Mo(NHBu^t)_2(NBu^t)_2]$ with $MeAlCl_2$. $[Mo(NHBu^t)_2(NBu^t)_2]$ (**6**) (50 mg, 0.13 mmol) was dissolved in C_6D_6 (0.8 mL), $MeAlCl_2$ (29 mg, 0.26 mmol) added and the reaction monitored by ^1H NMR spectroscopy, which indicated the quantitative formation of **7**.

Reaction of [Mo(NHBu^t)$_2$(N–2,6-Pr$^i_2$–C$_6$H$_3$)$_2$] with MeAlCl$_2$. [Mo(NHBu^t)$_2$(N–2,6-Pr$^i_2$–C$_6$H$_3$)$_2$] (**5**) (50 mg, 0.08 mmol) was dissolved in C$_6$D$_6$ (0.8 mL), MeAlCl$_2$ (19 mg, 0.17 mmol) added and the reaction monitored by ^{1}H NMR spectroscopy, which indicated the quantitative formation of [MoMe$_2$(N–2,6-Pr$^i_2$–C$_6$H$_3$)$_2$].[53]

[MoMe$_2$(N{2,6-Pr$^i_2$–C$_6$H$_3$}AlMe$_2${μ-Cl})(N–2,6-Pr$^i_2$–C$_6$H$_3$)] (8). [MoCl$_2$(N–2,6-Pr$^i_2$–C$_6$H$_3$)$_2$(dme)] (**1**) (1.0 g, 1.64 mmol) was dissolved in hexane (30 mL) and a solution of Me$_3$Al (0.80 g, 11.11 mmol) in hexane (30 mL) was added. This resulted in the immediate formation of a dark brown solution. The reaction was allowed to proceed for 16 h, after which time the solution was filtered to remove insoluble Me$_3$Al·dme adducts. The resulting solution was then cooled (−35 °C), which led to the formation of a small quantity of brown precipitate (Me$_3$Al–dme by-product), which was again removed *via* filtration. Further concentration of the hexane solution resulted in precipitation of **8** as a yellow solid, which was collected by filtration and recrystallised from hexane; yield 230 mg (24%). ^{1}H NMR (C$_6$D$_6$, 200 MHz): δ 6.93 (6H, s, H$_{meta}$ and H$_{para}$), 3.53 (2H, septet $^3J_{\mathrm{HH}}$ = 6.8 Hz, CH$_3$C*H*), 2.59 (2H, septet $^3J_{\mathrm{HH}}$ = 6.6 Hz, CH$_3$C*H*), 1.64 (6H, s, MoC*H*$_3$), 1.17 (6H, d, $^3J_{\mathrm{HH}}$ = 6.8 Hz, C*H*$_3$CH), 1.02 (6H, d, $^3J_{\mathrm{HH}}$ = 6.8 Hz, C*H*$_3$CH), 0.87 (12 H, d, $^3J_{\mathrm{HH}}$ = 6.6 Hz, C*H*$_3$CH), −0.09 (6H, s, AlC*H*$_3$). ^{13}C{^{1}H} NMR (C$_6$D$_6$, 125.6 MHz): δ 154.0 (C$_{ipso}$), 150.0 (C$_{ortho}$), 140.6 (C$_{meta}$), 125.0 (C$_{para}$), 41.5 (Mo(*C*H$_3$)$_2$), 30.1 (CH$_3$*C*H), 28.7 (CH$_3$*C*H), 26.2 (*C*H$_3$CH), 24.2 (*C*H$_3$CH), −7.0 (Al*C*H$_3$). Anal. calcd for C$_{28}$H$_{46}$AlClMoN$_2$: C, 59.10; H, 8.15; N, 4.92. Found C, 59.28; H, 8.14; N, 5.10.

[MoMe$_2$(N{2,6-Pr$^i_2$–C$_6$H$_3$}AlCl$_2${μ-Cl})(N–2,6-Pr$^i_2$–C$_6$H$_3$)] (9). i) [MoCl$_2$(N–2,6-Pr$^i_2$–C$_6$H$_3$)$_2$(dme)] (**1**) (400 mg, 0.65 mmol) was dissolved in a minimal amount of toluene (20 mL), before addition of a solution of MeAlCl$_2$ (1.9 mL, 1.0 M in hexanes, 1.90 mmol). The reaction mixture was allowed to stir (16 h) before being filtered and the volatile components removed *in vacuo*. Recrystallisation from CH$_2$Cl$_2$ gave brown micro crystals of complex **9** of sufficient quality for single crystal X-ray diffraction analysis. However, ^{1}H NMR spectroscopy of the bulk reaction material consistently indicated the formation of multiple reaction products. Furthermore, all attempts to purify the bulk of the material by recrystallization repeatedly failed. Repetition of this procedure using a larger amount of **1** (3.0 g, 4.93 mmol) also failed to produce material of sufficient purity. **ii)** Addition of solid MeAlCl$_2$ (30 mg, 0.26 mmol) to a toluene solution (0.8 mL) of **1** (50 mg, 0.08 mmol) resulted in an immediate colour change to give a dark brown solution; which was then charged to a recrystallization tube. Over a 24 h period large red crystals of **9** evolved and were collected *via* filtration and then washed with hexane (3 × 2 mL). Dissolution of a sample of these crystals in C$_6$D$_6$ allowed **9** to be characterized using ^{1}H NMR spectroscopy; ^{1}H NMR (C$_6$D$_6$, 200 MHz): δ 6.90 and 6.79 (6H, aromatic), 3.70 (2H, septet, $^3J_{\mathrm{HH}}$ = 6.8 Hz, CH$_3$C*H*), 2.37 (2H, septet, $^3J_{\mathrm{HH}}$ = 6.8 Hz, CH$_3$C*H*), 1.67 (6H, s, MoC*H*$_3$), 1.33 (6H, d, $^3J_{\mathrm{HH}}$ = 6.8 Hz, C*H*$_3$CH), 0.98 (6H, d, $^3J_{\mathrm{HH}}$ = 7 Hz, C*H*$_3$CH), 0.82 (12H, d, $^3J_{\mathrm{HH}}$ = 6.6 Hz, C*H*$_3$CH). Complex **9** degrades slowly both in the solid state and solution, which precluded acquisition of meaningful ^{13}C NMR spectroscopic and analytical data.

[MoMe$_2$(N{2,6-Pr$^i_2$–C$_6$H$_3$}AlMe$_2${μ-Cl})(NBu^t)] (10). [MoCl$_2$(N–2,6-Pr$^i_2$–C$_6$H$_3$)(NBu^t)(dme)] (**3**) (75 mg, 0.14 mmol) was dissolved in C$_6$D$_6$ (0.8 mL) and to this solution was added Me$_3$Al (64 mg, 0.88 mmol). This resulted in the quantitative (by NMR spectroscopy) formation of complex **10**. ^{1}H (C$_6$D$_6$, 500 MHz): δ 6.92 (3H, br s, aromatic), 3.45 (2H, septet, $^3J_{\mathrm{HH}}$ = 6.9 Hz, CH$_3$C*H*), 1.39 (6H, s, MoC*H*$_3$), 1.19 (6H, d, $^3J_{\mathrm{HH}}$ = 6.9 Hz, C*H*$_3$CH), 1.18 (6H, d, $^3J_{\mathrm{HH}}$ = 6.9 Hz, C*H*$_3$CH), 0.84 (6H, s, CC*H*$_3$), −0.21 (6H, s, AlC*H*$_3$). ^{13}C{^{1}H} NMR (C$_6$D$_6$, 125.6 MHz): δ 156.0 (C$_{ipso}$), 140.4 (C$_{ortho}$), 127.2 (C$_{meta}$), 124.5 (C$_{para}$), 74.2 (N*C*CH$_3$), 39.3 (Mo*C*H$_3$), 28.6 (NC*C*H$_3$), 28.2 (CH$_3$*C*H), 25.8 (*C*H$_3$CH), 25.0 (*C*H$_3$CH), and −6.7 (Al*C*H$_3$). In a ^{1}H–^{1}H NOESY spectrum of the reaction solution revealed a correlation between the C*H*$_3$CH (^{i}Pr) resonances and Al(C*H*$_3$)$_2$Cl resonances.

[MoMe$_2$(N{2,6-Pr$^i_2$–C$_6$H$_3$}AlCl$_2${μ-Cl})(NBu^t)] (11). [MoCl$_2$(N–2,6-Pr$^i_2$–C$_6$H$_3$)(NBu^t)(dme)] (**3**) (800 mg, 1.58 mmol) was dissolved in toluene (30 mL) and a hexane solution of MeAlCl$_2$ (4.8 mL, 1 M in hexanes, 4.76 mmol) was added. The reaction was allowed to stir for 16 h, after which time the solution was filtered. Concentration of the toluene solution followed by cooling (−5 °C) gave an initial crop of yellow micro crystals of complex **11** that were of sufficient quality for X-ray diffraction. After collection of the micro crystals the toluene washings were concentrated *in vacuo* resulting in further precipitation of complex **11**, which was collected *via* filtration and washed with hexane (3 × 5 mL). This material was then recrystallized from CH$_2$Cl$_2$ to give a yellow powder, yield 330 mg (40%): ^{1}H NMR (C$_6$D$_6$, 500 MHz): δ 6.90 (3H, s, H$_{meta}$ and H$_{para}$), 3.63 (2H, septet, $^3J_{\mathrm{HH}}$ = 7.0 Hz, CH$_3$C*H*), 1.38 (6H, s, MoC*H*$_3$), 1.32 (6H, d, $^3J_{\mathrm{HH}}$ = 7.0 Hz, C*H*$_3$CH), 1.11 (6H, d, $^3J_{\mathrm{HH}}$ = 7.0 Hz, C*H*$_3$CH), 0.68 (9H, s, NCC*H*$_3$).^{13}C{^{1}H} NMR (C$_6$D$_6$, 125.6 MHz): δ 154.5 (C$_{ipso}$), 140.9 (C$_{ortho}$), 128.1 (C$_{meta}$), 124.9 (C$_{para}$), 76.3 (N*C*CH$_3$), 45.1 (Mo*C*H$_3$), 28.6 (CH$_3$*C*H), 28.1 (NC*C*H$_3$), 25.7 (*C*H$_3$CH), 25.3 (*C*H$_3$CH). Anal. calcd for C$_{18}$H$_{33}$AlCl$_3$MoN$_2$: C, 42.66; H, 6.56; N, 5.53. Found: C, 42.87; H, 6.47; N, 5.56.

[MoMe$_2$(thf)(N–2,6-Pr$^i_2$–C$_6$H$_3$)$_2$] (12). [MoMe$_2$(N{2,6-Pr$^i_2$–C$_6$H$_3$}AlMe$_2${μ-Cl})(N–2,6-Pr$^i_2$–C$_6$H$_3$)] (**8**) (50 mg, 0.07 mmol) was dissolved in C$_6$D$_6$ (0.8 mL) and thf (28 μL, 0.35 mmol) added. Subsequently, the reaction was monitored by ^{1}H NMR spectroscopy, which indicated the quantitative formation of [MoMe$_2$(thf)(N–2,6-Pr$^i_2$–C$_6$H$_3$)$_2$] (**12**) together with a broad resonance from the aluminium-containing fragment.[53]

[MoMe$_2$(PMe$_3$)(N–2,6-Pr$^i_2$–C$_6$H$_3$)$_2$] (13). [MoMe$_2$(N{2,6-Pr$^i_2$–C$_6$H$_3$}AlMe$_2${μ-Cl})(N–2,6-Pr$^i_2$–C$_6$H$_3$)] (**8**) (50 mg, 0.07 mmol) was dissolved in C$_6$D$_6$ (0.8 mL) and PMe$_3$ (0.1 mL, 1.10 mmol) added *via* vacuum transfer at −196 °C. Following warming to r.t., the reaction was monitored by ^{1}H and ^{31}P NMR spectroscopy, which indicated the quantitative formation of [MoMe$_2$(PMe$_3$)(N–2,6-Pr$^i_2$–C$_6$H$_3$)$_2$] (**13**) together with broad resonances from the aluminium-containing residues.[53]

Reaction of [MoMe$_2$(N{2,6-Pr$^i_2$–C$_6$H$_3$}AlMe$_2${μ-Cl})(N–2,6-Pr$^i_2$–C$_6$H$_3$)] (8) with NEt$_3$. [MoMe$_2$(N{2,6-Pr$^i_2$–C$_6$H$_3$}

Table 3 Crystal data and experimental details

	5	**9**	**11**
Chemical formula	$C_{32}H_{54}MoN_4$	$C_{26}H_{40}AlCl_3MoN_2\cdot½CH_2Cl_2$	$C_{18}H_{32}AlCl_3MoN_2$
Fw	590.73	652.33	505.73
T/K	120	120	125
Crystal system	Orthorhombic	Monoclinic	Monoclinic
Space group (no.)	$Pbca$ (# 61)	$P2_1/n$ (# 14, non-standard)	$P2_1/c$ (# 14)
a/Å	10.463(1)	16.424(2)	9.046(1)
b/Å	19.225(2)	19.713(2)	16.394(2)
c/Å	33.429(3)	39.485(4)	16.605(2)
β (°)	90.00	97.22(1)	101.76(1)
V/Å^3	6724(1)	12683(2)	2587.3(4)
Z, ρ_c/g cm^{-3}	8, 1.167	16, 1.367	4, 1.393
μ/mm^{-1}	0.41	0.80	0.92
No. of reflns, total	71726	68331	28594
No. of reflns, unique	8928, 6757[a]	22278, 11385[a]	6418, 5474[a]
R_{int}	0.047	0.119	0.035
R_1[a,b]	0.033	0.066	0.025
wR_2[c]	0.079	0.135	0.066

[a] reflections with $I \geq 2\sigma(I)$; [b] $R_1 = \Sigma||F_o| - |F_c||/\Sigma|F_o|$; [c] $wR_2 = \{\Sigma[w(F_o^2 - F_c^2)^2]/\Sigma[w(F_o^2)^2]\}^{1/2}$.

$AlMe_2\{\mu\text{-}Cl\})(N\text{–}2,6\text{-}Pr^i_2\text{–}C_6H_3)]$ (**8**) (50 mg, 0.07 mmol) was dissolved in C_6D_6 (0.8 mL) and NEt_3 (50 μL, 0.35 mmol) added. Following warming to r.t., the reaction was monitored by ^{1}H NMR spectroscopy, which indicated the quantitative formation of $[MoMe_2(N\text{–}2,6\text{-}Pr^i_2\text{–}C_6H_3)_2]$ together with a broad resonance from the aluminium-containing fragment.[53]

Reaction of $[MoMe_2(N\{2,6\text{-}Pr^i_2\text{–}C_6H_3\}AlMe_2\{\mu\text{-}Cl\})(N\text{–}2,6\text{-}Pr^i_2\text{–}C_6H_3)]$ (8) with C_2H_4. $[MoMe_2(N\{2,6\text{-}Pr^i_2\text{–}C_6H_3\}AlMe_2\{\mu\text{-}Cl\})(N\text{–}2,6\text{-}Pr^i_2\text{–}C_6H_3)]$ (**8**) (50 mg, 0.08 mmol) was dissolved in C_6D_6 (0.8 mL) and the solution cooled (−196 °C), evacuated, and ethylene (10 equiv., 0.80 mmol) added, which lead to the formation of butenes according to ^{1}H NMR spectroscopy.

X-Ray crystallography

X-Ray diffraction experiments (Table 3) were carried out on Bruker 3-circle diffractometers with CCD area detectors ProteumM APEX (for **5**) or SMART 1000 (for **9** and **11**), using graphite-monochromated Mo-Kα radiation (λ = 0.71073 Å) from a 60 W Mo-target microfocus Bede Microsource® X-ray generator with glass polycapillary X-ray optics (**5**) or a sealed tube (**9**, **11**). The crystals were cooled using Cryostream 600 (Oxford Cryosystems) open-flow N_2 cryostats. Full sphere of the reciprocal space was covered with narrow-frame (0.3°) ω scans. Diffraction from **9** was very weak, mean $I/\sigma(I)$ = 4.2. Reflection intensities were corrected for absorption by semi-empirical method based on Laue equivalents.[58] The structures were solved by direct methods and refined by full-matrix least squares against F^2 of all reflections, using SHELXTL 6.14,[59] PLATON[60] and OLEX2[61] software. In the crystal of **9**, two independent CH_2Cl_2 molecules of crystallisation occupied voids of 133 and 185 Å^3, respectively. The latter molecule showed chaotic disorder, which could not be modelled satisfactorily, therefore the refinement was completed with the observed structure factors corrected using BYPASS procedure.[62] Full crystallographic data, excluding structure factors, have been deposited at the Cambridge Crystallographic Data Centre, CCDC-852768 (**5**), CCDC-852769 (**9**), and 852770 (**11**).

Acknowledgements

Durham University and Sasol Technology UK Ltd. (studentships WRHW and AMM) are warmly acknowledged for financial support of this work. We thank Dr A. M. Kenwright, Mrs. C. Heffernan, and Mr I. McKeag for assistance with NMR studies.

Notes and references

‡ For the preparation of complexes **7–10** excess alkyl aluminium reagent is required since the corresponding dme adduct of Me_xAlCl_{3-x} (x = 1 or 3) is obtained in each case; such species have been reported previously.[63]

1 J. Skupińska, *Chem. Rev.*, 1991, **91**, 613.
2 D. Vogt, in *Applied Homogeneous Catalysis with Organometallic Compounds*, 2nd Edtn., B. Cornils and W. A. Herrmann, ed., Wiley-VCH, Weinheim, Germany, 2002, Vol. 1, pp. 240–253.
3 A. Forestière, H. Olivier-Bourbigou and L. Saussine, *Oil Gas Sci. Technol.*, 2009, **64**, 649.
4 D. W. Lee and C. S. Yi, *Organometallics*, 2010, **29**, 3413.
5 S. Muthukumaru Pillai, M. Ravindranathan and S. Sivaram, *Chem. Rev.*, 1986, **86**, 353.
6 J. T. Dixon, M. J. Green, F. M. Hess and D. H. Morgan, *J. Organomet. Chem.*, 2004, **689**, 3641.
7 H. Olivier-Bourbigou and L. Saussine, in *Applied Homogeneous Catalysis with Organometallic Compounds*, 2nd Edtn., B. Cornils and W. A. Herrmann, ed., Wiley-VCH, Weinheim, Germany, 2002, Vol. 1, pp. 253–265.
8 G. R. Lappin and J. D. Sauer, *Alpha-Olefins Applications Handbook*, Marcel Decker Inc., Berkeley, CA, 1989.
9 G. R. Lappin, L. H. Nemec, J. D. Sauer and J. D. Wagner, Higher Olefins, in *Kirk-Othmer Encyclopedia of Chemical Technology*, Wiley & Sons, New York, 2005.
10 A. M. Al-Jarallah, J. A. Anabtawi, M. A. B. Siddiqui, A. M. Aitani and A. W. Al-Sa'doun, *Catal. Today*, 1992, **14**, 1.
11 D. S. McGuinness, *Chem. Rev.*, 2011, **111**, 2321.
12 P. W. N. M. van Leeuwen, N. D. Clement and M. J.-L. Tschan, *Coord. Chem. Rev.*, 2011, **255**, 1499.

13 M. Marchionna, M. Di Girolamo and R. Patrini, *Catal. Today*, 2001, **65**, 397.

14 F. Speiser, P. Braunstein and L. Saussine, *Acc. Chem. Res.*, 2005, **38**, 784.

15 R. M. Manyik, W. E. Walker and T. P. Wilson, *J. Catal.*, 1977, **47**, 197.

16 J. R. Briggs, *J. Chem. Soc., Chem. Commun.*, 1989 (11), 674.

17 R. M. Manyik, W. E. Walker and T. P. Wilson, US 3300458 (Union Carbide Corporation), 1967

18 T. Agapie, *Coord. Chem. Rev.*, 2011, **255**, 861.

19 D. F. Wass, *Dalton Trans.*, 2007, 816.

20 W. K. Reagan, EP 0417477 (Phillips Petroleum Company), 1991

21 A. Jabri, C. B. Mason, Y. Sim, S. Gambarotta, T. J. Burchell and R. Duchateau, *Angew. Chem., Int. Ed.*, 2008, **47**, 9717.

22 L. McDyre, E. Carter, K. J. Cavell, D. M. Murphy, J. A. Platts, K. Sampford, B. D. Ward, W. F. Gabrielli, M. J. Hanton and D. M. Smith, *Organometallics*, 2011, **30**, 4505.

23 W. A. Nujent and J. M. Mayer, *Metal–Ligand Multiple Bonds*, Wiley-Inter Science, New York, 1988.

24 (*a*) D. S. Williams, M. H. Schofield, J. T. Anhaus and R. R. Schrock, *J. Am. Chem. Soc.*, 1990, **112**, 6728; (*b*) P. W. Dyer, V. C. Gibson, J. A. K. Howard, B. Whittle and C. Wilson, *J. Chem. Soc., Chem. Commun.*, 1992, 1666.

25 M. P. Coles, C. I. Dalby, V. C. Gibson, W. Clegg and M. R. J. Elsegood, *J. Chem. Soc., Chem. Commun.*, 1995, 1709.

26 M. P. Coles and V. C. Gibson, *Polym. Bull.*, 1994, **33**, 529.

27 H. Olivier and O. Laurent-Gérot, *J. Mol. Catal. A: Chem.*, 1999, **148**, 43.

28 W. R. H. Wright, A. S. Batsanov, J. A. K. Howard, R. P. Tooze, M. J. Hanton and P. W. Dyer, *Dalton Trans.*, 2010, **39**, 7038.

29 (*a*) H. R. Menapace, G. S. Benner and N. A. Maly, (Goodyear) U.S. Pat. 3,784, 629-3,784,631, 1972; (*b*) G. W. Lawson, (Goodyear) U.S. Pat. 3,813,453, 1974; (*c*) N. A. Maly, H. R. Menapace and G. S. Benner, (Goodyear) U.S. Pat. 3,903,193, 1975.

30 H. R. Menapace, N. A. Maly, J. L. Wang and L. G. Wideman, *J. Org. Chem.*, 1975, **40**, 2983.

31 D. E. Hendriksen, (Exxon) U.S. Pat. 5,059,739, 1991

32 M. J. Hanton, L. Daubney, T. Lebl, S. Polas, D. M. Smith and A. Willemse, *Dalton Trans.*, 2010, **39**, 7025.

33 M. J. Hanton, R. P. Tooze, (Sasol Technology UK) WO2005089940, 2005

34 R. R. Schrock, *Chem. Rev.*, 2009, **109**, 3211.

35 J. C. Mol, *J. Mol. Catal. A: Chem.*, 2004, **213**, 39.

36 H. H. Fox, K. B. Yap, J. Robbins, S. Cai and R. R. Schrock, *Inorg. Chem.*, 1992, **31**, 2287.

37 H. H. Fox, K. B. Yap, J. Robbins, S. Chai and R. R. Schrock, *Inorg. Chem.*, 1992, **31**, 2287.

38 P. W. Dyer, V. C. Gibson and W. Clegg, *J. Chem. Soc., Dalton Trans.*, 1995, 3313.

39 P. Barrie, J. A. Coffey, G. D. Forster and G. Hogarth, *J. Chem. Soc., Dalton Trans.*, 1999, 4519.

40 A. Bell, W. Clegg, P. W. Dyer, M. R. J. Elsegood, V. C. Gibson and E. L. Marshall, *J. Chem. Soc., Chem. Commun.*, 1994, 2547.

41 P. W. Dyer, V. C. Gibson, J. A. K. Howard, B. Whittle and C. Wilson, *Polyhedron*, 1995, **14**, 103.

42 W. R. H. Wright, A. S. Batsanov, J. A. K. Howard, R. P. Tooze, M. J. Hanton and P. W. Dyer, *unpublished work.*.

43 R. Ramnauth, S. Al-Juaid, M. Motevalli, B. C. Parkin and A. C. Sullivan, *Inorg. Chem.*, 2004, **43**, 4072.

44 A. A. Danopoulos, G. Wilkinson, B. Hussain-Bates and M. B. Hursthouse, *J. Chem. Soc., Dalton Trans.*, 1990, 2753.

45 W. A. Nugent and R. L. Harlow, *J. Am. Chem. Soc.*, 1980, **102**, 1759.

46 (*a*) N. Bryson, M.-T. Youinou and J. A. Osborn, *Organometallics*, 1991, **10**, 3389; (*b*) T. Chen, K. R. Sorasaenee, Zh. Wu, J. B. Diminnie and Z. Xue, *Inorg. Chim. Acta*, 2003, **345**, 113.

47 For representative examples see: (*a*) V. C. Gibson, C. Redshaw, W. Clegg and M. R. J. Elsegood, *J. Chem. Soc., Dalton Trans.*, 1997, 3207; (*b*) R. R. Schrock, J. Y. Jamieson, J. P. Araujo, P. J. Bonitatebus Jnr., A. Sinha and L. P. H. Lopez, *J. Organomet. Chem.*, 2003, **684**, 56; (*c*) S. Cai, R. R. Schrock, R. R. Kempe and W. M. Davis, *Polyhedron*, 1998, **17**, 749; (*d*) A. Majumdar and S. Sarkar, *Inorg. Chim. Acta*, 2009, **362**, 3493; (*e*) D. Morales, J. Perez, L. Riera, V. Riera, D. Miguel, M. E. G. Mosquera and S. Garcia-Grande, *Chem.–Eur. J.*, 2003, **9**, 4132; (*f*) L. Y. Kuo, M. G. Kanatzidis, M. Sabat, A. L. Tipton and T. J. Marks, *J. Am. Chem. Soc.*, 1991, **113**, 9027; (*g*) A. Anillo, R. Obeso-Rosete, M. Lanfranchi and A. Tiripicchio, *J. Organomet. Chem.*, 1993, **453**, 71.

48 The structure of **5** may be related to that for valence isoelectonic and isolable bent Group 4 metallocene complexes [Cp$_2$M(NR$_2$)$_2$]; see: (*a*) P. W. Dyer, V. C. Gibson, J. A. K. Howard, B. Whittle and C. Wilson, *J. Chem. Soc., Chem. Commun.*, 1992, 1666; (*b*) D. S. Williams, M. H. Schofield, J. T. Anhaus and R. R. Schrock, *J. Am. Chem. Soc.*, 1990, **112**, 6728.

49 J. W. Lauher and R. Hoffmann, *J. Am. Chem. Soc.*, 1976, **98**, 1729.

50 V. C. Gibson, *J. Chem. Soc., Dalton Trans.*, 1994, 1607.

51 W. A. Nugent, R. J. McKinney, R. V. Kasowski and F. A. Van-Catledge, *Inorg. Chim. Acta*, 1982, **65**, L91.

52 (*a*) S. Tobisch, *Proc. Comp. Sci.*, 2011, **4**, 1203; (*b*) S. Tobisch, *Dalton Trans.*, 2008, 2120.

53 V. C. Gibson, C. Redshaw, G. L. P. Walker, J. A. K. Howard, V. J. Hoy, J. M. Cole, L. G. Kuzmina and D. S. De Silva, *J. Chem. Soc., Dalton Trans.*, 1999, 161.

54 S. Alvarez, P. Alemany, D. Cassanova, J. Cirera, M. Llunell and D. Avnir, *Coord. Chem. Rev.*, 2005, **249**, 1693.

55 (*a*) R. Harrison, A. M. Arif, G. Wulsberg, R. Lang, T. Ju, G. Kiss, C. D. Hoff and T. G. Richmond, *J. Chem. Soc., Chem. Commun.*, 1992, 1374; (*b*) Z. J. Tonzetich, A. J. Jiang, R. R. Schrock and P. Muller, *Organometallics*, 2006, **25**, 4725.

56 V. C. Gibson, E. L. Marshall, C. Redshaw, W. Clegg and M. R. J. Elsegood, *J. Chem. Soc., Dalton Trans.*, 1996, 4197.

57 R. C. B. Copley, P. W. Dyer, V. C. Gibson, J. A. K. Howard, E. L. Marshall, W. Wang and B. Whittle, *Polyhedron*, 1996, **15**, 3001.

58 G. M. Sheldrick, *SADABS 2.10*, Bruker AXS, Madison WI, USA, 2003

59 G. M. Sheldrick, *Acta Crystallogr., Sect. A: Found. Crystallogr.*, 2008, **64**, 112.

60 A. L. Spek, *Acta Crystallogr., Sect. D: Biol. Crystallogr.*, 2009, **65**, 148–155.

61 O. V. Dolomanov, L. J. Bourhis, R. J. Gildea, J. A. K. Howard and H. Puschmann, *J. Appl. Crystallogr.*, 2009, **42**, 339.

62 P. van der Sluis and A. L. Spek, *Acta Crystallogr., Sect. A: Found. Crystallogr.*, 1990, **46**, 194–201.

63 N. C. Means, C. M. Means, S. G. Bott and J. L. Atwood, *Inorg. Chem.*, 1987, **26**, 1466.